Tropical tropospheric ozone: Implications for dynamics and biomass burning

S. Chandra,[1] J. R. Ziemke,[2] P. K. Bhartia,[1] and R. V. Martin[3]

Received 7 February 2001; revised 19 June 2001; accepted 6 September 2001; published 17 July 2002.

[1] This paper studies the significance of large-scale transport and pyrogenic (i.e., biomass burning) emissions in the production of tropospheric ozone in the tropics. Using aerosol index (AI) and tropospheric column ozone (TCO) time series from 1979 to 2000 derived from the Nimbus-7 and Earth Probe Total Ozone Mapping Spectrometer measurements, our study shows significant differences in the seasonal and spatial characteristics of pyrogenic emissions north and south of the equator in the African region and Brazil in South America. Notwithstanding these differences, most of the observed seasonal characteristics are well simulated by the GEOS-CHEM global model of tropospheric chemistry. The only exception is the northern African region where modeled and observed TCO differ significantly. In the Indonesian region the most significant increase in TCO occurred during September–December 1997, following large-scale forest and savanna fires associated with the El Niño induced dry condition. The increase in TCO extended over most of the western Pacific well outside the burning region and was accompanied by a decrease in the eastern Pacific resembling a west-to-east dipole about the dateline. These features are well simulated in the GEOS-CHEM model which suggests that both the biomass burning and changes in meteorological conditions during the El Niño period contributed almost equally to the observed increase in TCO in the Indonesian region. During 1997 the net increase in TCO integrated over the tropical region between 15°N and 15°S was about 6–8 Tg (1 Tg = 10^{12} g) over the mean climatological value of about 77 Tg. The GEOS-CHEM model suggests that most of this increase may have been caused by biomass burning in the Indonesian region since dynamical components of El Niño induced changes in TCO tend to cancel out in the area-averaged data. In addition to biomass burning, the interannual variability in the area-averaged column ozone in the tropics is influenced by a number of factors including the quasi-biennial oscillation and solar cycle. *INDEX TERMS:* 3374 Meteorology and Atmospheric Dynamics: Tropical meteorology; 0305 Atmospheric Composition and Structure: Aerosols and particles (0345, 4801); 0365 Atmospheric Composition and Structure: Troposphere—composition and chemistry; 0368 Atmospheric Composition and Structure: Troposphere—constituent transport and chemistry; *KEYWORDS:* biomass burning, tropospheric ozone, El Niño, solar cycle, quasi-biennial oscillation

1. Introduction

[2] It is generally recognized that pyrogenic (i.e., biomass burning) emissions produced by the forest and savanna fires in southern Africa and Brazil are a significant source of ozone-producing precursor gases which may produce 10–15 Dobson unit (DU) increases in tropospheric column ozone (TCO) in the South Atlantic region during austral spring (see, e.g., *Fishman et al.* [1996], *Thompson et al.* [1996], *Jacob et al.* [1996], and several related papers in the special issue "South Tropical Atlantic Regional Experiment (STARE): Transport and Atmospheric Chemistry Near the Equator–Atlantic (TRACE-A) and Southern African Fire-Atmosphere Research Initiative (SAFARI)" of the *Journal of Geophysical Research*, *101*(D19), 23,519–24,330, 1996). However, recent studies based on three-dimensional (3-D) atmospheric chemistry and transport models suggest that the photochemical O_3 formation from biomass burning may be less important than was indicated in previous studies [e.g., *Lelieveld and Dentener*, 2000; *Marufu et al.*, 2000; *Moxim and Levy*, 2000]. The significance of biomass burning in producing seasonal and zonal anomalies in ozone in the tropics was recently discussed by *Ziemke and Chandra* [1999] based on 20 years (1979–1998) of TCO time series derived from the convective cloud differential (CCD) method using total ozone mapping spectrometer (TOMS) version 7 retrievals. Their study showed that the amplitude of the annual cycle in the South Atlantic region peaks at about the same time (September and October) from 15°N to 15°S even though the biomass burning in the African region occurs at different times over north and south of

[1]NASA Goddard Space Flight Center, Greenbelt, Maryland, USA.
[2]Stinger Ghaffarian Technologies Inc., Greenbelt, Maryland, USA.
[3]Division of Engineering and Applied Sciences, Harvard University, Cambridge, Massachusetts, USA.

0148-0227/02/2001JD000447$09.00

the equator. Such a phase lag was not observed following the large-scale burning of forest fires in the tropical rain forest of Kalimantan and Sumatra during the El Niño of 1997–1998. During September 1997, when the forest fires were most intense in this region, the TCO increased to about 40–50 DU without any significant phase lag [*Chandra et al.*, 1998; *Ziemke and Chandra*, 1999]. These values were comparable to values usually observed in the South Atlantic region. In fact, the increase in TCO after the Indonesian fires was not limited to this region but extended over thousands of kilometers from the southern part of India in the northern hemisphere to Fiji in the south, and far eastward to Samoa in the southeast, east of the dateline. Recently, *Thompson et al.* [2001] have reported similar results based on tropospheric column ozone derived from TOMS data using a modified residual method. The question if such a widespread increase in TCO was caused by forest fires over Kalimantan and Sumatra covering a relatively small area of about 45,600 km^2 or by changes in large-scale transport induced by the 1997 El Niño is of considerable importance in understanding the significance that biomass burning has in the photochemical formation of O_3 in the troposphere.

[3] The effect of Indonesian fires on tropospheric ozone was estimated by *Hauglustaine et al.* [1999] using a global chemical transport model. Using emission rates of ozone precursor gases given by *Levine et al.* [1999], they estimated an increase of 20–25 DU in TCO over source regions (Sumatra and Kalimantan), in general agreement with the estimates given by *Chandra et al.* [1998]. However, the estimated ozone amount outside the source region was significantly lower. It is difficult to estimate the temporal and long-range implications of these calculations since dynamical conditions prevailing during the El Niño of 1997 were not taken into account.

[4] The 1997 El Niño event was unique since the unusual forest fires in Indonesia were preceded by the normal burning seasons in Brazil and southern Africa. The purpose of this paper is to study the possible role of these events on tropospheric ozone which was significantly elevated for several months over half the tropical belt encompassing South America, southern Africa, and Indonesia. Our study is based on nearly 22 years [1979–2000] of TCO time series derived from the CCD method by combining Nimbus-7 and Earth Probe version 7 TOMS data. During the 1997 El Niño period a number of ozonesondes in different regions of the tropics were operating under the Southern Hemisphere Additional Ozonesondes (SHADOZ) program which was initiated by NASA Goddard Space Flight Center in 1998 with the participation of a number of U.S. and international investigators [*Thompson et al.*, 2002]. The ozone profiles from some of these regions are used in this study for cross validation with the CCD data and for inferring relative changes in the upper and lower troposphere during the El Niño period. The biomass burning events are inferred from the TOMS aerosol smoke index (AI) [*Hsu et al.*, 1996]. The relative contributions of biomass burning and transport on tropospheric column ozone and ozone profile are estimated using the GEOS-CHEM global 3-D model of tropospheric chemistry and transport driven by assimilated meteorological fields during the 1996–1997 period [*Bey et al.*, 2001a].

2. Aerosol Smoke Index (AI)

[5] The biomass burning events are generally inferred from the fire count maps derived from the Along Track Scanning Radiometer (ATSR) night images (http:// shark1.esrin.esa.it/ionia/FIRE/AF/ATSR). We have used the TOMS aerosol index as a proxy for biomass burning because it also represents biomass burning and, more importantly, it has the same temporal and spatial coverage as TCO. AI is calculated from the ratio of a pair of ultraviolet wavelengths measured from TOMS instruments as follows [*Hsu et al.*, 1996, 1999]:

$$\mathrm{AI} = -100[\log_{10}(I_{340}/I_{380})_{\mathrm{meas}} - \log_{10}(I_{340}/I_{380})_{\mathrm{calc}}], \quad (1)$$

where $(I_{340}/I_{380})_{\mathrm{meas}}$ is the ratio of the backscattered radiances at 340 and 380 nm measured by TOMS and $(I_{340}/I_{380})_{\mathrm{calc}}$ is the corresponding values calculated from a radiative transfer model for a pure Rayleigh-scattering atmosphere. The positive and negative values of AI generally correspond to absorbing and non-absorbing aerosols at UV wavelengths, respectively. The wavelengths used in equation (1) apply to Nimbus 7 TOMS measurements. For the Earth Probe TOMS instrument the 340 nm wavelength is replaced by 331 nm, and 380 nm is replaced by 360 nm.

[6] Both the CCD and AI data used in this study are monthly averages with a horizontal resolution of 5° by 5° within the latitude range 15°S–15°N (centered on latitudes 12.5°S, 7.5°S, and 12.5°N). There is a large gap of missing CCD and AI data from May 1993 through June 1996 because there were no applicable TOMS satellite measurements during this time period. Although the Meteor-3 TOMS instrument made measurements from late August 1991 to December 1994, the non-Sun-synchronous orbit of the satellite created high solar zenith angles in the tropics which generated a large amount of spurious CCD TCO measurements.

3. GEOS-CHEM Atmospheric Chemistry and Transport Model

[7] The GEOS-CHEM model [*Bey et al.*, 2001a], a three-dimensional global atmospheric chemistry and transport model, is used to simulate the tropical tropospheric ozone distribution. The model is driven by assimilated meteorological data, updated every 3 hours, from the Global Earth Observing System (GEOS) of the NASA Data Assimilation Office (DAO) [*Schubert et al.*, 1993]. The model version used here has 26 vertical levels on a sigma coordinate (surface to 0.1 hPa), and a horizontal resolution of 4° latitude by 5° longitude. The model includes a detailed description of tropospheric ozone-NO_x-hydrocarbon chemistry. It solves the chemical evolution of about 120 species with a Gear solver [*Jacobson and Turco*, 1994] and transports 24 tracers. Photolysis rates are computed using the Fast-J radiative transfer algorithm [*Wild et al.*, 2000] which includes Rayleigh scattering and Mie scattering by clouds and mineral dust. Emissions of NO_x from lightning are

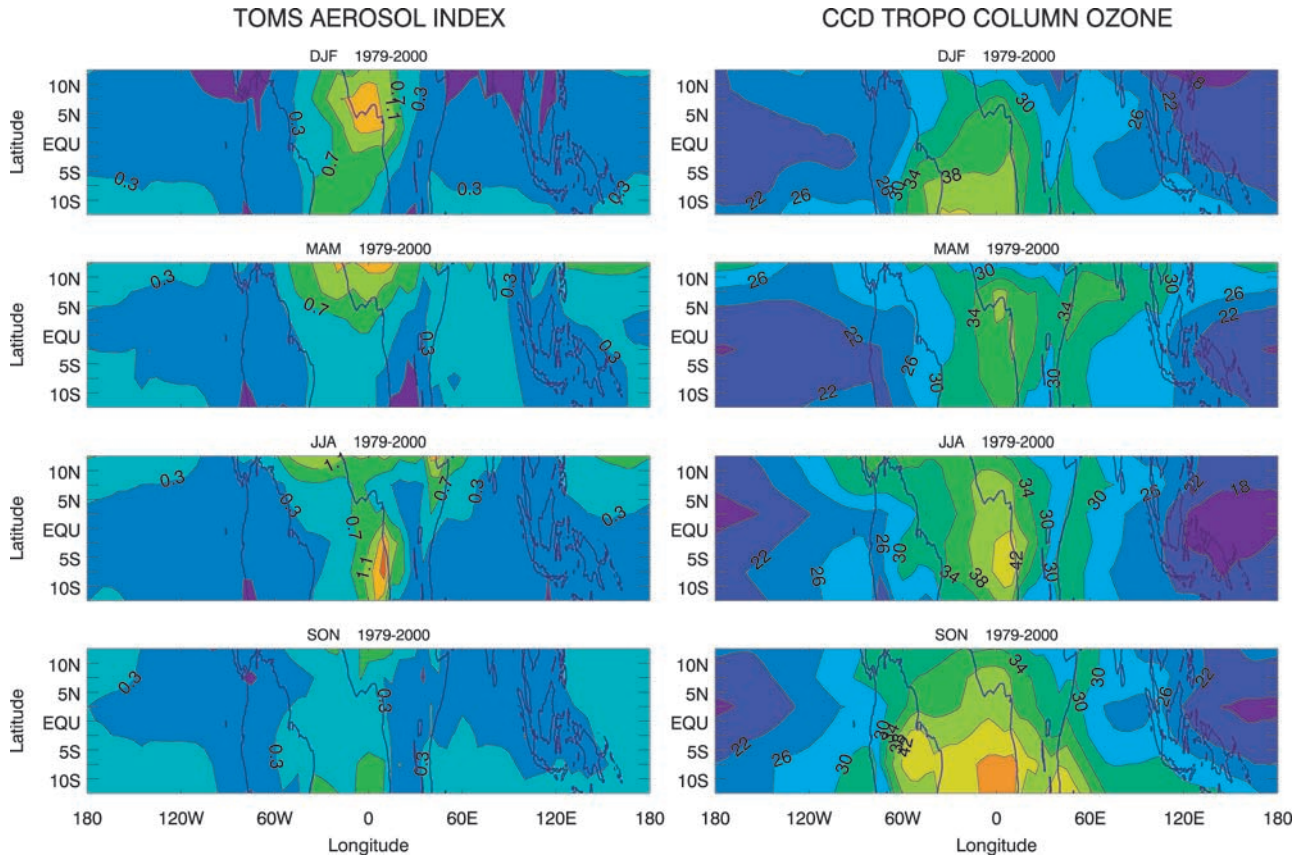

Figure 1. (left) TOMS aerosol index (no units) seasonal climatology. The data shown were determined by averaging over 3-month seasons (indicated) for the time period 1979–2000. (right) Same as the left-hand frames, but for TOMS CCD tropospheric total column ozone (in Dobson units).

linked to deep convection following the parameterization of *Price and Rind* [1992] as implemented by *Wang et al.* [1998]. Biogenic isoprene and NO_x emissions from land are computed locally using modified versions of the *Guenther et al.* [1995] and *Yienger and Levy* [1995] algorithms, as described by *Wang et al.* [1998] and *Bey et al.* [2001a]. Extensive evaluations of the GEOS-CHEM chemical fields with observations are presented in a number of papers [*Bey et al.*, 2001a, 2001b; *Fiore et al.*, 2002; *Kondo et al.*, 2002; *Li et al.*, 2000, 2002; *Liu et al.*, 2001; *Palmer et al.*, 2001; *Singh et al.*, 2000; R. V. Martin et al., manuscript in preparation, 2001]. This simulation includes updates as described by R. V. Martin et al. (manuscript in preparation, 2001). The most important updates are improved biomass burning and biofuels emission climatologies (R. Yevich and J. Logan, personal communication, 2001) and the determination of seasonal and interannual variation in biomass burning emissions from satellite observations (B. N. Duncan et al., manuscript in preparation, 2001) which has been applied to 10 species including NO and CO. The interannual variation in biomass burning emissions over Oceania is of particular interest here. B. N. Duncan et al. (manuscript in preparation, 2001) estimate this variation from 15 years of AI and 3 years of global fire counts from the Along Track Scanning Radiometer (ATSR) World Fire Atlas [*Arino and Rosaz*, 1999]. They scale the monthly regional emissions to the normalized interannual AI variation in which the AI background and enhancements from volcanic eruptions were removed. The resulting emissions from Oceania in September and October 1997 are 0.52 and 0.36 Tg N, respectively, compared with 0.02 Tg N in September and October 1996. They map the emissions onto the GEOS-CHEM grid according to the number of ATSR fire counts in each grid square for each month. The interannual variation in biomass burning emissions is being used in model studies of aerosol emissions [*Chin et al.*, 2002], pollution transport from Asia (A. C. Staudt et al., Sources and chemistry of nitrogen oxides over the tropical Pacific, submitted to *Journal of Geophysical Research*, 2002), and tropical tropospheric ozone (R. V. Martin et al., manuscript in preparation, 2001).

4. TCO and AI Climatologies

[8] Figure 1 shows zonal variations in AI (left) and TCO (right) climatology in the tropics based on 22 years of data from 1979 through 2000. A number of corrections have been applied in deriving TCO from the CCD method including adjustments for tropospheric aerosols, a partial correction for sea glint (bright surface reflection) errors, an ozone retrieval efficiency correction for the lower troposphere, and an instrument calibration offset correction between Nimbus 7 and Earth probe TOMS. Details of these corrections are discussed by *Ziemke et al.* [2000] and

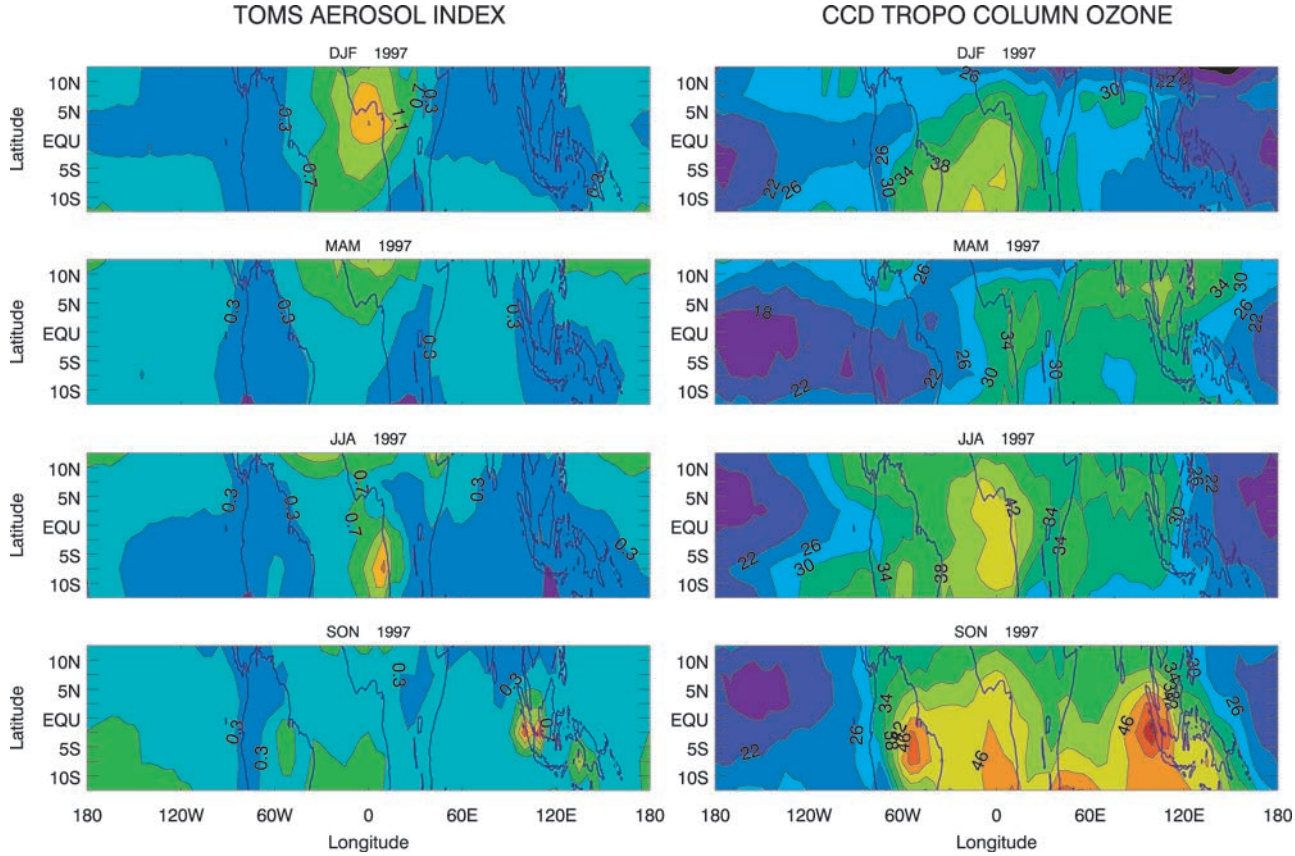

Figure 2. Same as Figure 1, but for the year 1997 instead of climatology.

[2001]. In Figure 1 the four panels on each side are averages of the months December-January-February (DJF), March-April-May (MAM), June-July-August (JJA), and September-October-November (SON). These seasonal averages represent winter (summer), spring (fall), summer (winter), and fall (spring) conditions of the northern (southern) hemisphere. The seasonal and zonal characteristics of TCO inferred from Figure 1 are similar to the ones discussed by *Ziemke and Chandra* [1999], a predominantly zonal asymmetry feature in all seasons with maximum in the Atlantic and minimum in the Pacific region. The seasonality in the Pacific region is generally weak. It is stronger in the Atlantic region with minimum (30–35 DU) in MAM and maximum (40–45 DU) in SON seasons. The amplitude of the seasonal cycle in the Atlantic region increases from about 3 DU north of the equator to about 6 DU south of equator. Assuming that AI values less than 0.6 are statistically not significant [e.g., *Hsu et al.*, 1999], Figure 1 suggests that the African region is the major source of aerosols. Unfortunately, the AI measurement does not always indicate the presence of carbonaceous aerosol produced by biomass burning. *Hsu et al.* [1999] showed that the derived AI is linearly proportional to aerosol optical thickness (AOT) derived independently from ground-based Sun photometers over regions of biomass burning and regions covered by African dust. *Hsu et al.* [1999] suggested that the high values of AI (>0.7) in summer (Figure 1, third panel) are caused by savanna burnings in southern Africa. In northern Africa, high values of AI (Figure 1, first and second panels) are associated with both the desert dust and biomass burning. This picture is generally consistent with the monthly mean fire count map derived from ATSR night images (not shown). Figure 1 suggests an apparent relation between AI and TCO south of the equator in the southern African region. TCO increased at about the same time as AI in JJA. However, TCO continued to increase over a much wider region extending to South America in the west and the Indian Ocean in the east well after the JJA enhancement in AI.

[9] In general, TCO peaks in September–October, about 2 months after AI reaches peak values around July–August over most of the regions in southern Africa. Such a phase relation is not indicated in regions north of the equator. AI in northern Africa is strongly influenced by desert mineral dust from Saharan and Sahel dust storms and does not necessarily indicate the presence of carbonaceous aerosols. Relatively high values of TCO from the western coast of Africa to the eastern coast of South America (Figure 1, top panel) thus do not seem to be related to AI. *Thompson et al.* [2000] have characterized this apparent anomaly as the "tropical Atlantic paradox." A lack of correlation between TCO and AI is also apparent in Brazil. The climatological values of AI in this region when averaged over the 3-month SON period are statistically not significant even though the TCO field over the same period is almost as robust as over the African region. A weaker AI field in Brazil appears to be in contradiction with the satellite fire count data in this region and may be caused by meteorological conditions in

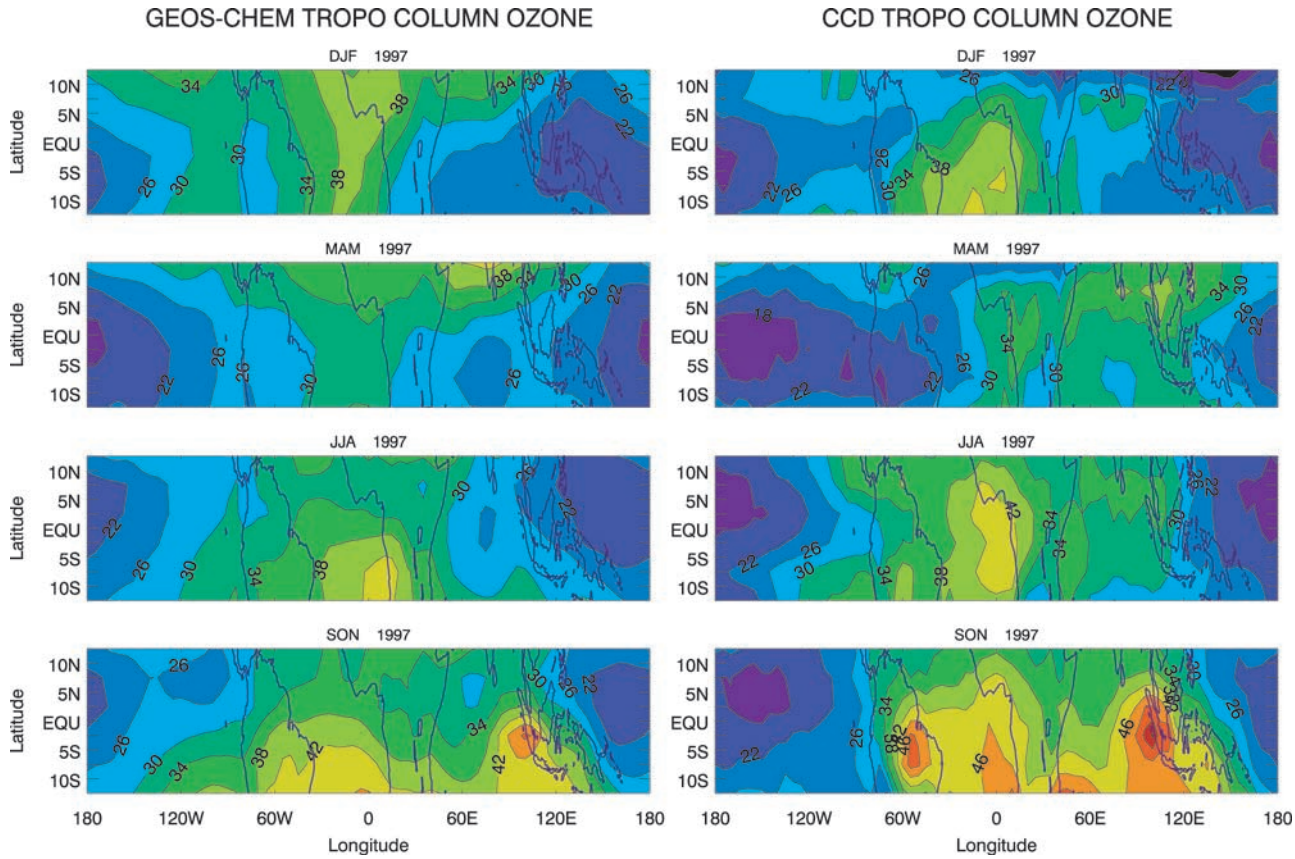

Figure 3. Zonal and seasonal variation in TCO for the year 1997 based on GEOS-CHEM model (left-hand side) compared with observations (right-hand side). The latter is identical to Figure 2 (right-hand side).

this region which are not the same as in southern Africa. This dependence on meteorological conditions may limit the usefulness of AI as a tracer of biomass burning plumes [*Fenn et al.*, 1999]. Unfortunately, AI is the only global index available over the entire period of TOMS measurements.

5. TCO Field During 1997 El Niño

[10] The basic patterns of TCO and AI fields shown in Figure 1 do not change significantly from year to year except during El Niño years which are accompanied by a change in the convection pattern and biomass burning in the Indonesian region. This is seen in Figure 2 which shows AI and TCO fields for 1997. The two fields are very similar to climatological fields as in Figure 1 except in the Indonesian region. The latter shows a significant increase in AI during September and October encompassing the islands of Sumatra and Borneo (Figure 2, left, fourth panel) associated with the biomass burning in this region. The corresponding increase in TCO after the Indonesian fires is not limited to this region but extends over thousands of kilometers from southern India in the north, to Fiji in the south, and eastward as far as Samoa. The highest TCO values are in the range of 50–55 DU and are coincident with the regions of biomass burning in Sumatra and Borneo. These features are well simulated in the GEOS-CHEM model. Figure 3 compares the modeled TCO fields for 1997 for the four seasons (left-hand side) with observations (right-hand side). The latter is the same as in Figure 2 (left-hand side) and is reproduced in Figure 3 for visual comparison. The model seems to capture most of the seasonal and spatial characteristics of observed TCO including the El Niño related enhancement in TCO in the Indonesian region. The seasonal characteristics of the model and observations, however, differ significantly north of the equator. This is more clearly seen in Figure 4 which compares the temporal variations in TCO derived from the CCD and the GEOS-CHEM model over the 15-month period from September 1996 to November 1997. This comparison is made over both north and south of the equator in three regions of the tropics, eastern Pacific, Atlantic/African, and western Pacific/Indonesian. As seen in Figure 4, the model captures the temporal variations in TCO over most of the regions of the tropics, particularly south of the equator. The agreement is remarkably good in the Indonesian region (Figure 4f) and the African region south of the equator (Figure 4e). Both the model and observations show a sharp rise in TCO in the Indonesian region after August 1997 following the large-scale forest and savanna fires in this region. The model also captures the observed seasonality in TCO south of the equator (Figure 4e). The model and observations, however, differ significantly north of the equator in the African region (Figure 4b). The observed TCO tends to have a broad peak

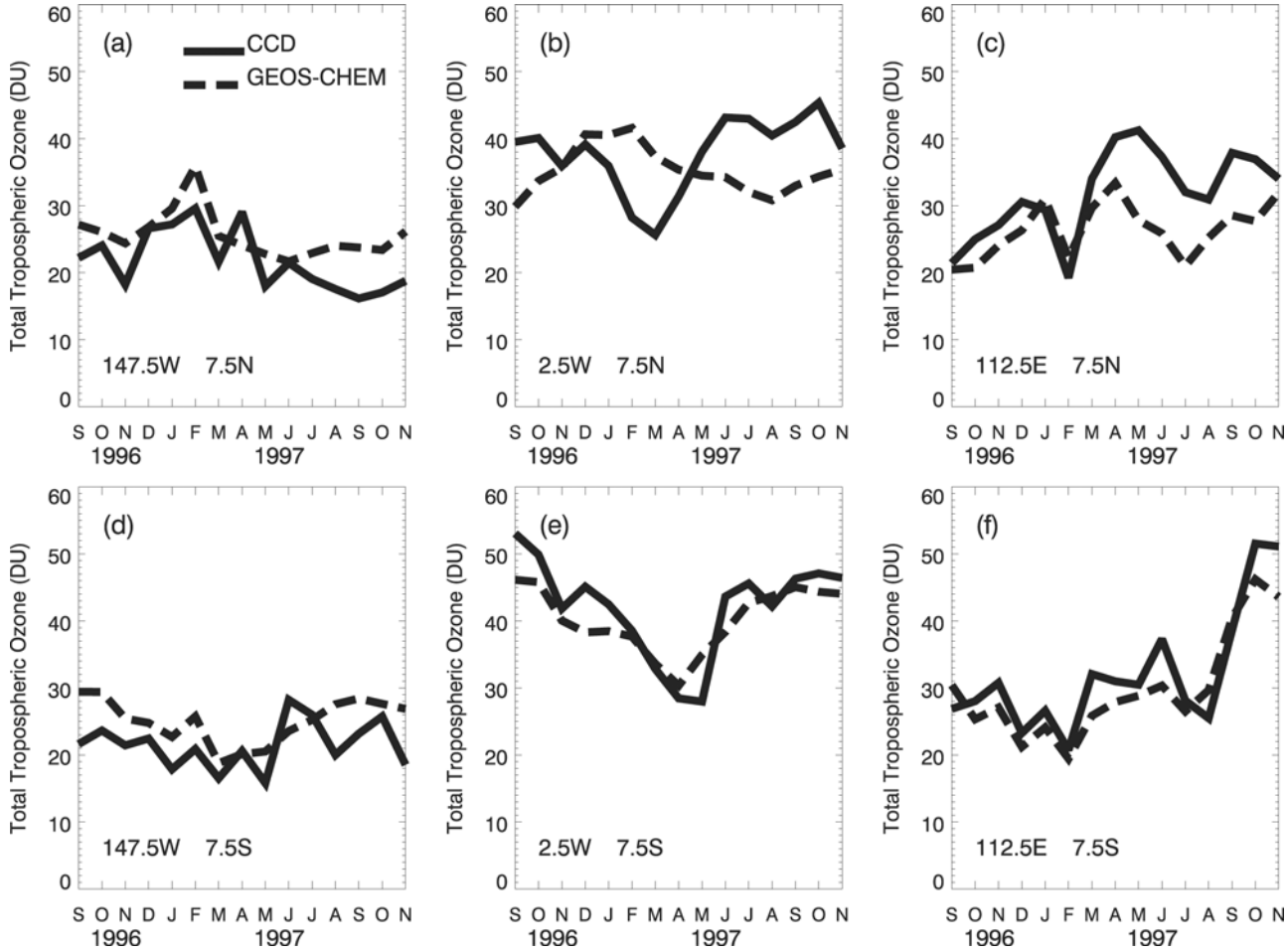

Figure 4. Comparison of seasonal and temporal variations in TCO derived from the CCD and the GEOS-CHEM model over the 15-month period of simulation from September 1996 to November 1997. This comparison is made over both north and south of the equator in three regions of the tropics: (a and d) eastern Pacific, (b and e) Atlantic/African, and (c and f) western Pacific/Indonesian.

in late fall (September–November) and a minimum in early spring (February–March) similar to TCO seasonality south of the equator (Figure 4e). The model phase is just the opposite and seems to be consistent with the burning season in northern Africa as inferred from the AI index (Figures 1 and 2, left-hand side). This apparent discrepancy between model and observations is not understood and is discussed further by R. V. Martin et al. (manuscript in preparation, 2001).

6. Comparison With Ozonesondes

[11] The TCO, being a column ozone measurement, does not provide any information as to how different vertical regions of the troposphere were affected by biomass burning and large-scale transport during the 1997 El Niño. To validate the model vertical structure, GEOS-CHEM ozone fields are compared with ozonesonde measurements for the total tropospheric ozone column, and also the column ozone amount in the lower (below 500 hPa) and the middle and the upper (above 500 hPa) troposphere. Figures 5, 6 and 7 show the comparison of model results with column ozone derived from ozonesonde and CCD at three locations south of the equator. The first of these locations is Watukosek (8°S, 113°E) in eastern Java, just 5° south of Kalimantan (3°S, 113°E). The latter was the region of intense biomass burning during September–October 1997 (Figure 2, left-hand side). The ozonesonde data at Watukosek with respect to 1997 El Niño have been discussed in detail by *Fujiwara et al.* [1999, 2000]. The other two locations are Nairobi, Kenya (1°S, 37°E), a city situated near the equator in the African region but outside the main burning region in southern Africa (Figures 1 and 2, left-hand side), and Samoa (14°S, 171°W) in the South Pacific region farther away from all the burning sources. Though the CCD time series cover the time period of EP TOMS measurements beginning from August 1996 to the end of 2000, the model and ozonesonde measurements cover different time intervals during this period. All the time series overlap the 15-month period of GEOS-CHEM model simulation from September 1996 to November 1997.

[12] Figure 5a compares observed TCO from CCD and ozonesondes with the GEOS-CHEM model at Watukosek. Unfortunately, the ozonesonde time series is not continuous and has missing data for a few months during 1997. The model, nevertheless, generally captures the temporal changes

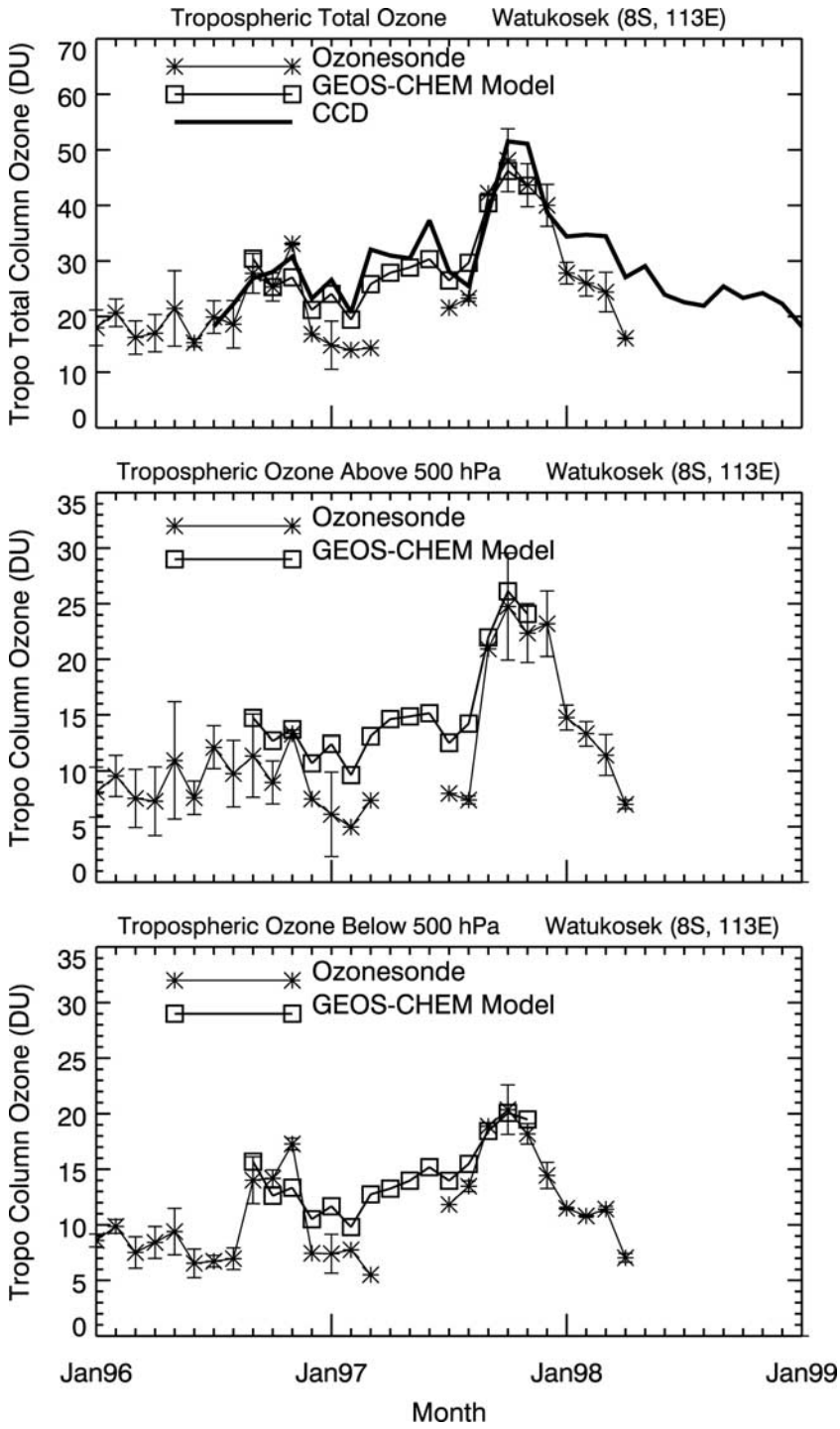

Figure 5. (top) Comparison of GEOS-CHEM model (squares) with tropospheric total column O_3 at Watukosek (8°S, 113°E) derived from ozonesonde (stars) and CCD method (solid line). (middle and bottom) Model comparison with ozone amount esimated from ozonesonde data above and below 500 hPa. Vertical bars for the ozonesonde data represent $\pm 1\sigma$ standard deviations.

in observed TCO including the rapid increase after August 1997. Both the model and measurements suggest peak values in TCO during September–October 1997. This increase is about 15–20 DU compared to a mean value of about 30 DU during October 1996. The model results are generally consistent with observed changes in ozone in both the upper and the lower troposphere (Figures 5b and 5c). It is interesting to note that most of this increase occurred in the upper troposphere (above 500 hPa) which is consistent with the downward motion in this region caused by the change in Walker circulation [*Chandra et al.*, 1998]. This feature was also noted by *Fujiwara et al.* [2000], who attributed the upper tropospheric ozone enhancement to transport of ozone from the troposphere and horizontal

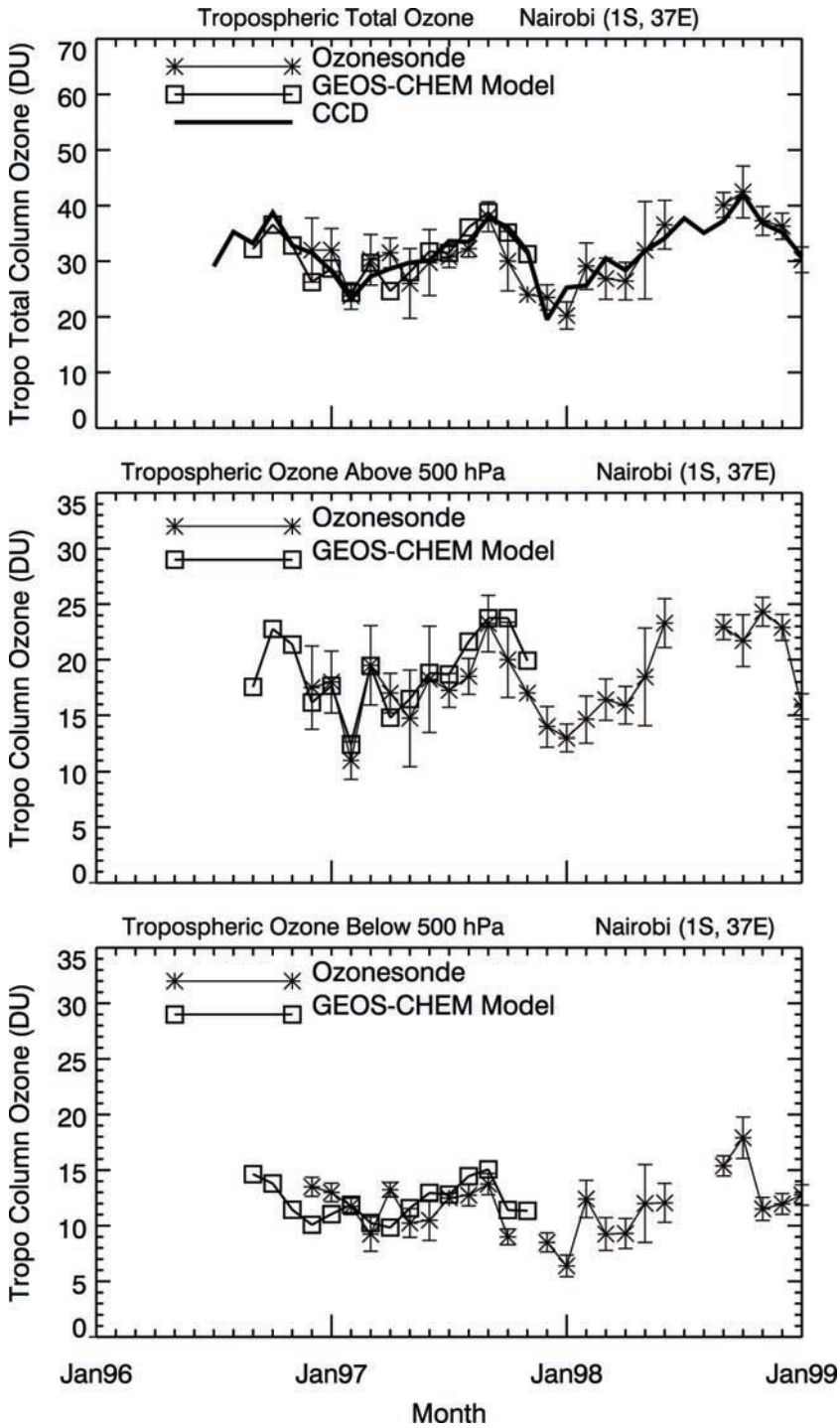

Figure 6. Same as Figure 5, but for Nairobi (1°S, 37°E).

transport of ozone-enriched air masses from the burning region west of Watukosek.

[13] At Nairobi (Figure 6a), CCD and ozonesonde time series are in remarkable agreement both with respect to their absolute values and temporal changes. They both show strong seasonal cycles with peak values of about 40 DU during September–October months, characteristic of the tropical Atlantic region. They agree remarkably well with the GEOS-CHEM model over the 15 months of the simulation. The model also represents the observed changes in TCO above and below 500 hPa (Figures 6b and 6c). Figure 7 compares TCO measured from ozonesondes with CCD-derived TCO at Samoa over the 1996–1998 time period. As in Figures 5 and 6, TCO derived from the two sets of measurements at this location are in good agreement and show similar seasonal and temporal variations within the uncertainty of the two sets of measurements. The seasonal cycles during 1996 and 1998 are essentially similar showing a steep rise from about 10–15 DU to about 20–25 DU during the early part of

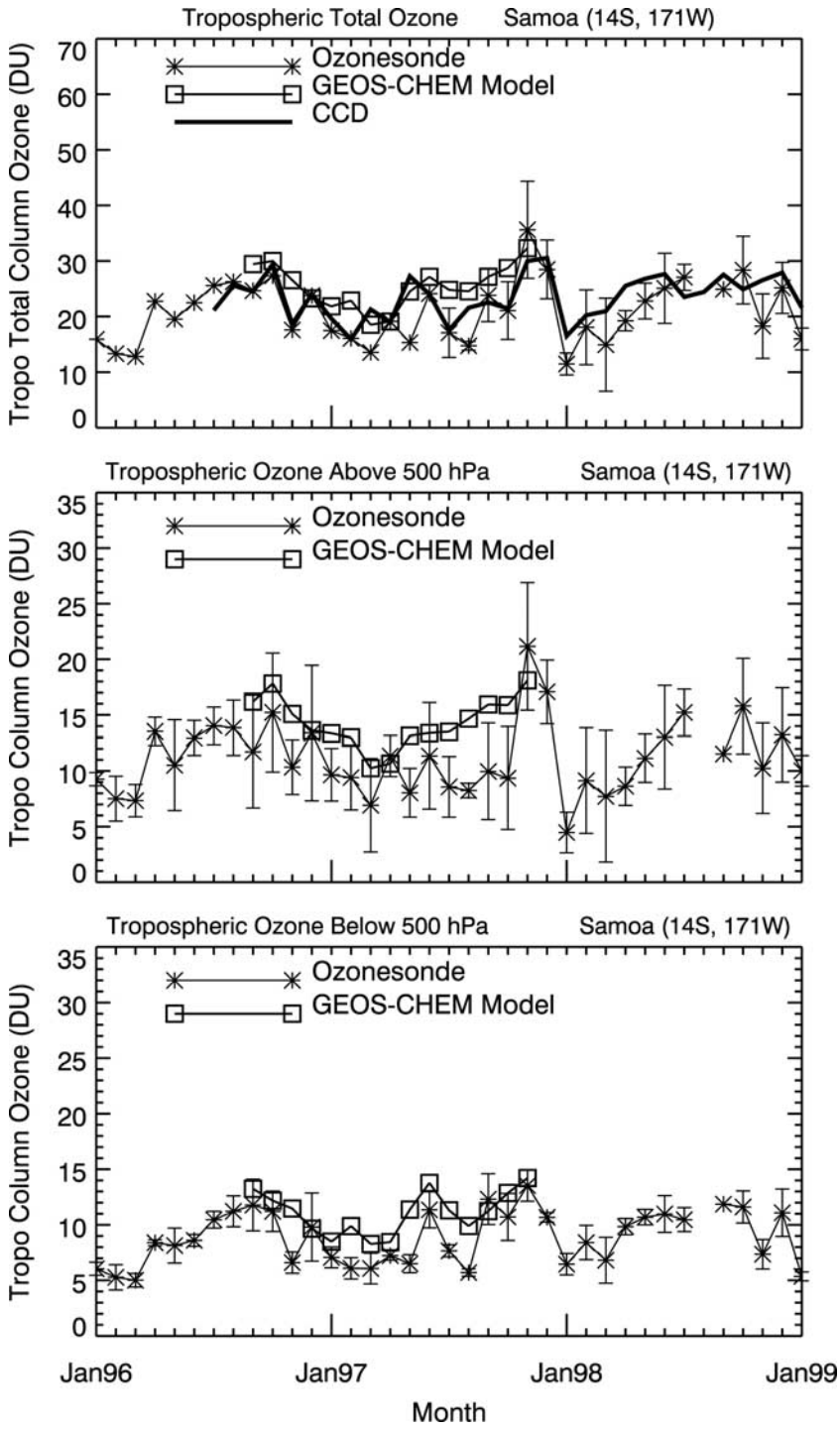

Figure 7. Same as Figure 5, but for Samoa (14°S, 171°W).

the year. In comparison, 1997 appears to be noisier. The model simulates most of these changes above and below 500 hPa as in Figures 5 and 6 but is generally high above 500 hPa.

7. Implications for Large-Scale Transport and Biomass Burning

[14] The ability of the GEOS-CHEM model to simulate the observed changes in ozone in the tropical troposphere enables one to study the relative importance of large-scale transport and biomass burning based on this model. Figures 8, 9, 10, 11, and 12 show zonal variations in AI and TCO in the tropics for years preceding (1996), during (1997), and after (1998) the El Niño episode which developed during March 1997 and strengthened rapidly over the following several months. To highlight the effect of tropical convection, the orientations of these figures, with respect to Figure 1, are shifted by 180° with the dateline (180° longitude) in the middle. Figure 8 shows

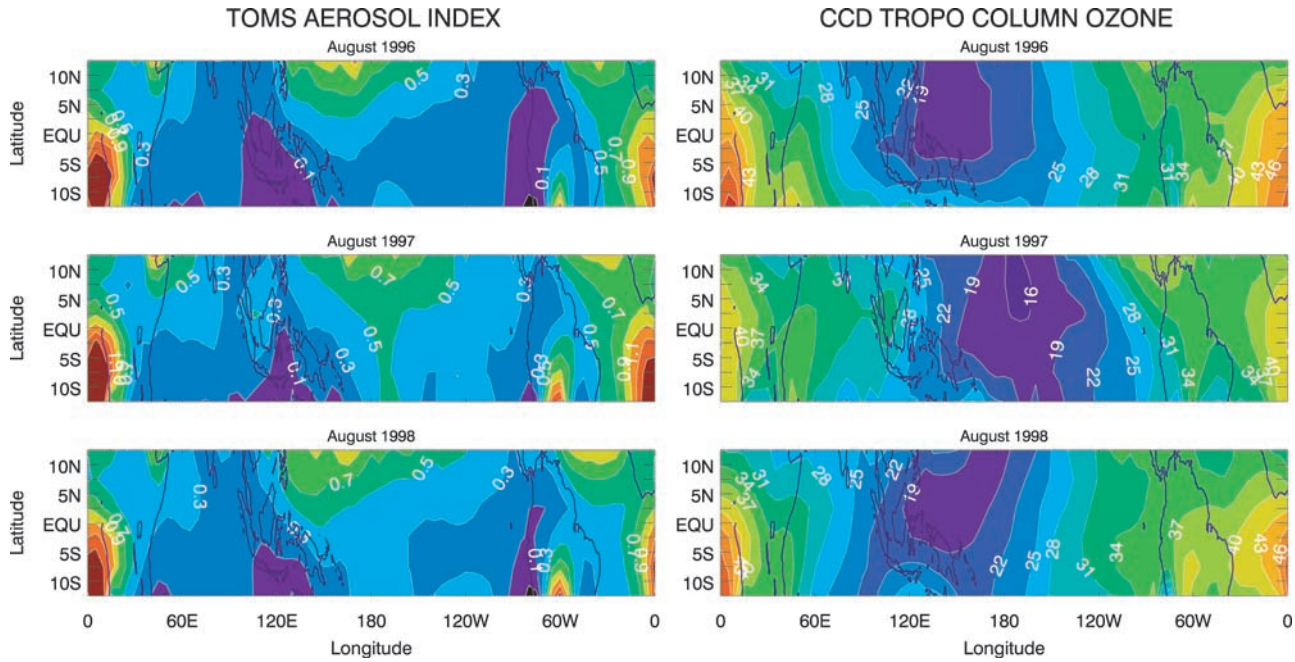

Figure 8. (left) TOMS aerosol index (no units) for (top) August 1996, (middle) August 1997, and (bottom) August 1998. (right) Same as left-hand frames, but for TOMS CCD tropospheric total column O_3 (in Dobson units). In contrast to Figures 1 and 2, the dateline (180°) is now shown in the middle of each frame.

these fields for the month of August. August 1997 preceded the onset of large-scale forest fires during September and October 1997 in the Indonesian region (Figures 9 and 10). The AI field in Figure 8 shows significant enhancement (>0.7) over a very large area in southern Africa and a similar increase in Brazil in South America but over a much smaller area. These increases are associated with the biomass burning in these regions. Though the general pattern of the AI field is similar in all 3 years, the TCO field in 1997 (Figure 8, middle panel) is significantly different compared to the preceding and the later years. The TCO field in August in all 3 years shows a characteristic zonal asymmetry with high values of 30–40 DU in the southern Atlantic region and low values in

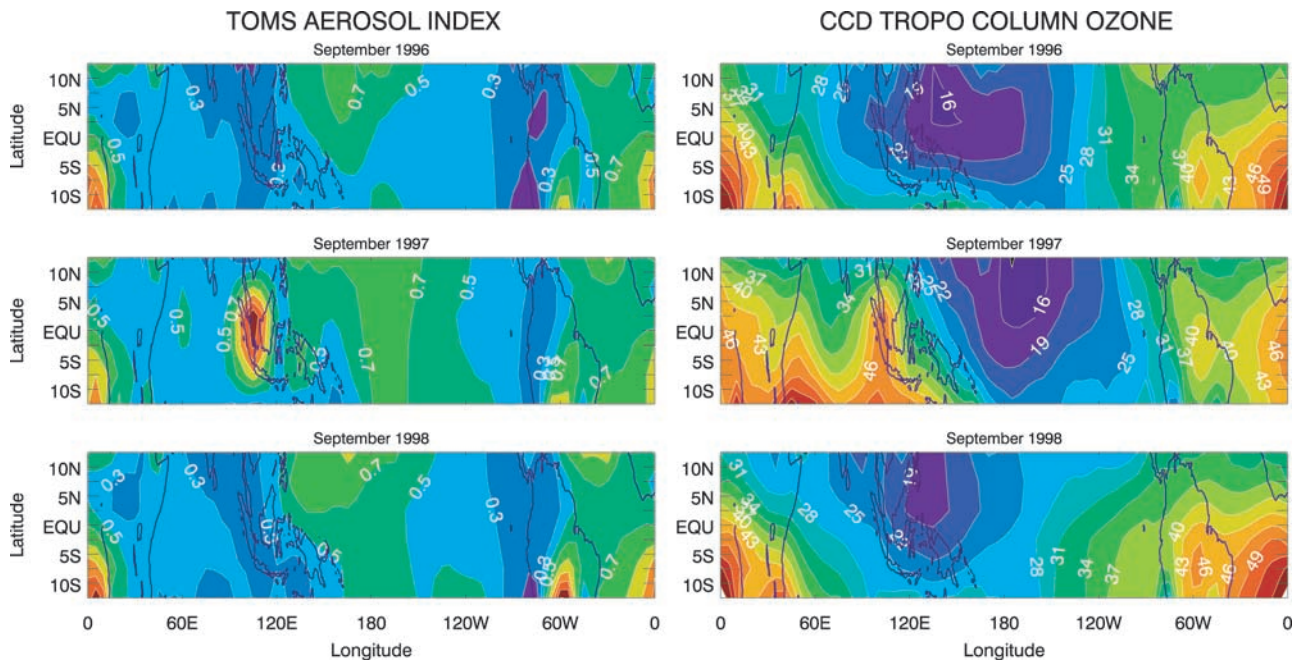

Figure 9. Same as Figure 8, but for September 1996–1998.

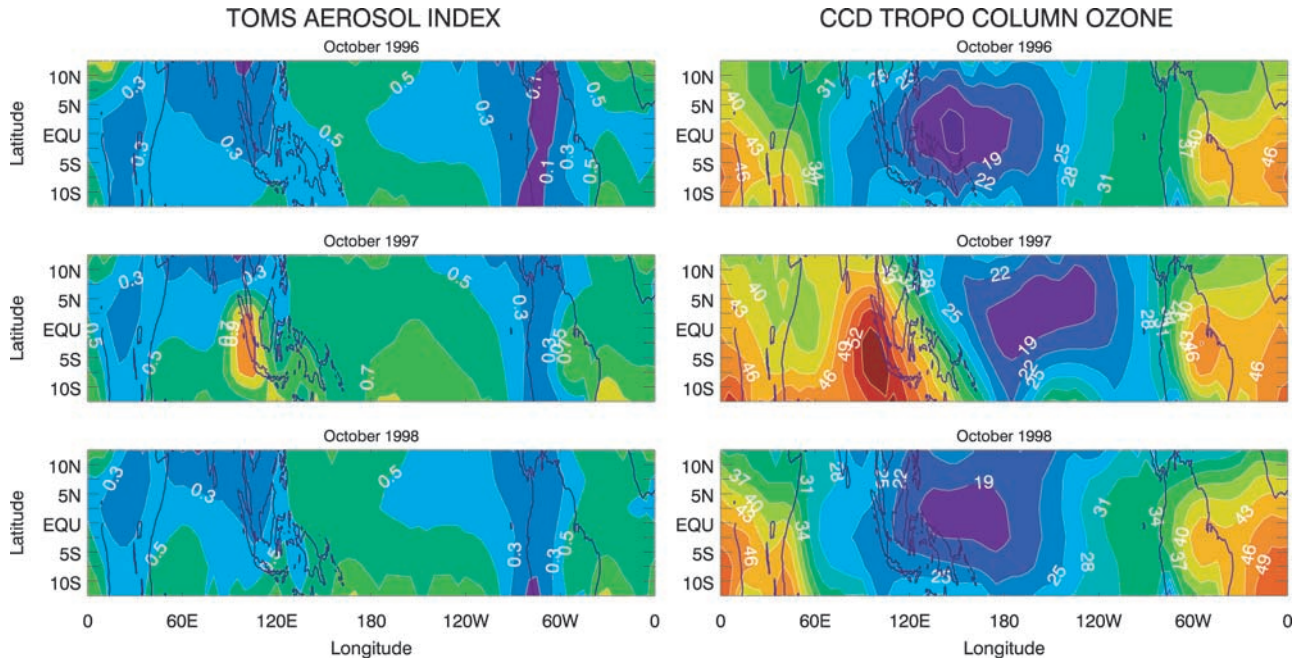

Figure 10. Same as Figure 8, but for October 1996–1998.

the Pacific region. During August 1997 the low region was shifted east of the dateline causing a decrease of 6–8 DU over most of the eastern Pacific region. An increase of about the same magnitude occurred over regions of the western Pacific including Indonesia. These positive and negative changes were almost entirely due to the shift in the convection pattern from the western to the eastern Pacific and the related changes in the tropical circulation as discussed *Chandra et al.* [1998]. With the intensification of El Niño the Indonesian region showed a rapid buildup of ozone over a considerably larger area than affected by forest fires (e.g., Figures 9 and 10, middle panels). However, the zonal contrast in TCO persisted over several months with significantly high values of TCO (40–50 DU) in the western Pacific well after the cessation of forest fires in the Indonesian region as seen in

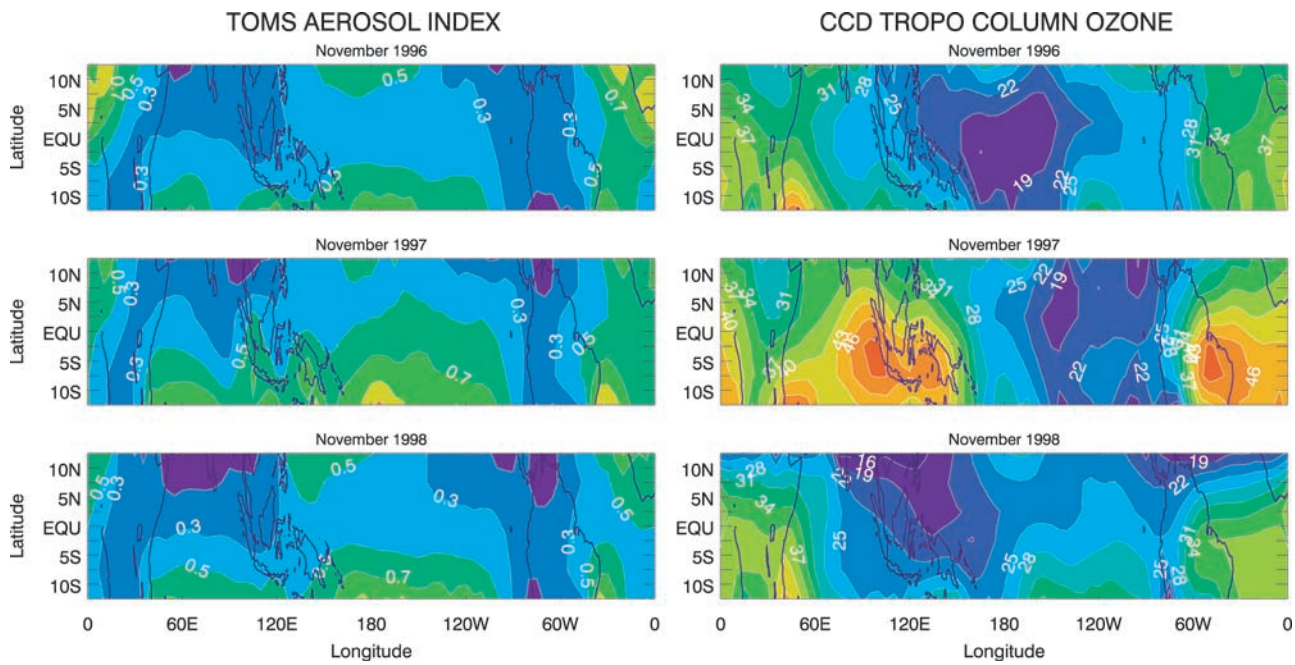

Figure 11. Same as Figure 8, but for November 1996–1998.

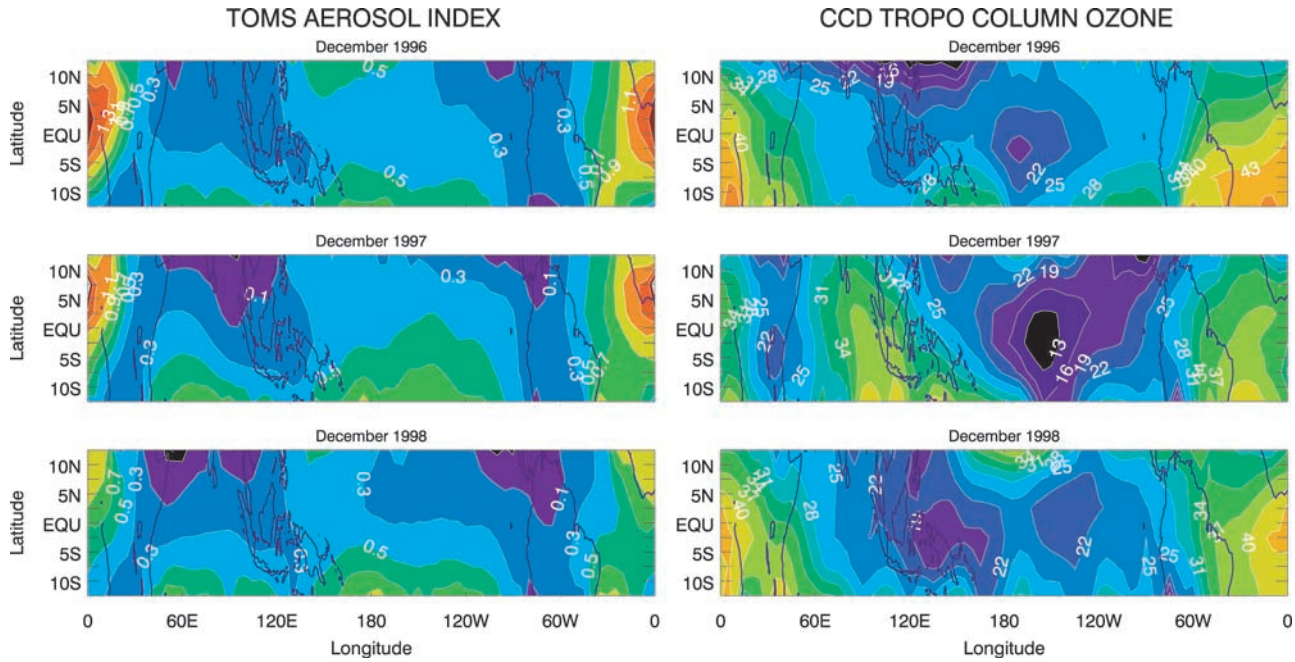

Figure 12. Same as Figure 8, but for December 1996–1998.

Figures 11 and 12 (middle panels). The GEOS-CHEM model captures most of the observed features in TCO and suggests that both the biomass burning and changes in large-scale transport during this period contributed almost equally to observed changes in TCO. This will be discussed in the following using October 1996 and 1997 as examples.

[15] Figure 13 compares the zonal anomalies in TCO derived from the CCD (top panel) and the model (bottom panel) in October 1997. The anomalies shown in this figure are relative changes in TCO with respect to October 1996. The model accounts for changes in meteorological conditions and biomass burning from Oceania during October 1996 to October 1997. The NO_x emission rates for these months are 0.02 and 0.36 Tg N, respectively. The observed anomalies are the differences in TCO fields as shown in the top and middle panels of Figure 10 (right-hand side) and are very similar to the ones reported by *Chandra et al.* [1998]. The differences from *Chandra et al.* [1998] are mainly due to a number of corrections applied to the CCD data in the current version. These corrections, as stated earlier, include adjustments for tropospheric aerosols, a partial correction for sea glint errors, and an ozone retrieval efficiency correction for the lower troposphere [*Ziemke et al.*, 2001]. As seen in Figure 13, the model reproduces the observed features remarkably well. Both the observed and simulated changes in TCO show an asymmetrical dipole in TCO with a negative anomaly of 2–8 DU over most of the eastern Pacific region and a positive anomaly of 4–28 DU over most of the western Pacific region. The higher positive values are generally associated with large-scale forest fires in the Indonesian region as inferred from the AI index (Figure 10, left-hand side). The peak values of the observed anomaly (24–28 DU) are higher by about 4 DU than the model values (20–24) but well within the uncertainty of both the modeled and CCD values. *Chandra et al.* [1998] suggested that the dipole nature of the observed anomaly in TCO is the manifestation of large-scale circulation associated with the shift in tropical convection and surface boundary layer processes associated with the forest fires in the Indonesian region.

[16] To assess the relative importance of these processes, the GEOS-CHEM model was run with two scenarios. The first one illustrates the difference between the standard simulation with enhanced biomass burning emissions over Oceania and a sensitivity simulation without biomass burning emissions (Figure 14, top panel). The second scenario portrays the effect of dynamical changes from October 1996 to October 1997 (Figure 14, bottom panel). A comparison of these simulations suggests that the dipole nature of the TCO anomaly is more symmetrical with respect to the dateline when only the meteorological processes are considered. The asymmetry is caused mostly by enhanced ozone due to biomass burning. The increase in TCO due to biomass burning is significantly greater (12–16 DU) in the areas mostly affected by biomass burning as inferred from the AI index (Figure 10, left-hand side). Outside this area the contributions due to biomass burning and transport are almost equal (4–8 DU). Using meteorological conditions prevailing during 1997, *Sudo and Takahashi* [2001] studied the effects of the 1997 El Niño event on tropospheric ozone using a 3-D photochemical model developed at the Center for Climate System Research, University of Tokyo, Japan. They were able to simulate most of the observed changes in tropospheric ozone reported by *Chandra et al.* [1998] and concluded, as in this paper, that both the biomass burning and the changes in meteorological conditions (e.g., low convective activity, sparse precipitation, dry air condition,

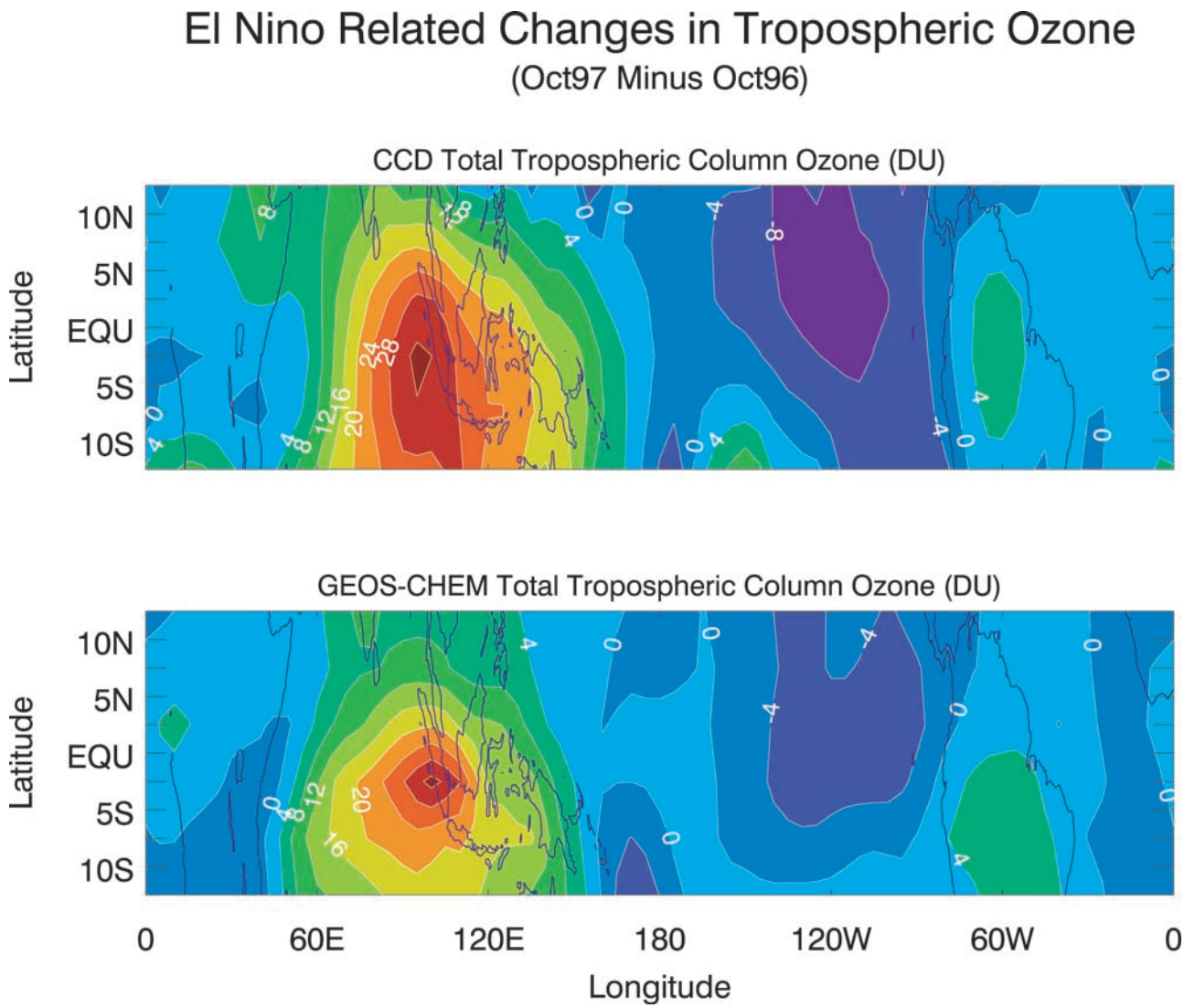

Figure 13. (top) TOMS CCD tropospheric total column O_3 anomaly field for October 1997 with respect to October 1996 (October 1997 to October 1996). The dateline is shown in the middle of the frame. (bottom) Similar to CCD anomaly field, but instead based on the GEOS-CHEM model.

large-scale dynamical changes) contributed almost equally to the observed enhancement in tropospheric ozone in the Indonesian region.

8. El Niño and Interannual Variability

[17] Since El Niño related dynamical changes in the tropical Pacific region produce both positive and negative anomalies, they tend to cancel each other in the zonally averaged data. It is therefore useful to integrate TCO over the tropical region and estimate the net increase in TCO which may be attributed to pyrogenic sources. Figure 15 compares the seasonal variation in TCO over the tropical region in 1997 with a climatology based on the 22 years (1979–2000) of the CCD database. Both data sets are area-averaged over the latitude band from 15°N to 15°S and are expressed in units of teragrams (Tg; 1 Tg = 10^{12} g) to reflect the ozone mass abundance in the tropical troposphere. Figure 15 indicates a clear seasonal pattern in TCO climatology with a mean value of about 77 Tg. This is about 3 times larger than the TCO abundance in the African region estimated by *Marufu et al.* [2000]. The TCO climatology has a relatively weaker peak in spring and a stronger peak in fall. These peaks are reflections of higher values of ozone in these months over the tropical Atlantic region encompassing most of southern Africa and Brazil (Figure 1). Compared to climatology, the TCO values over most of 1997 are elevated after the development of El Niño in March 1997. Some of these elevated values are associated with biomass burning in the Indonesian region. For example, during September and October 1997 when the biomass burning was most intense in the Indonesian region Figures 10 and 11, the TCO values were 10–12 Tg higher than climatology. These values are comparable to a similar enhancement seen during June and July 1997, long before the start of large-scale forest

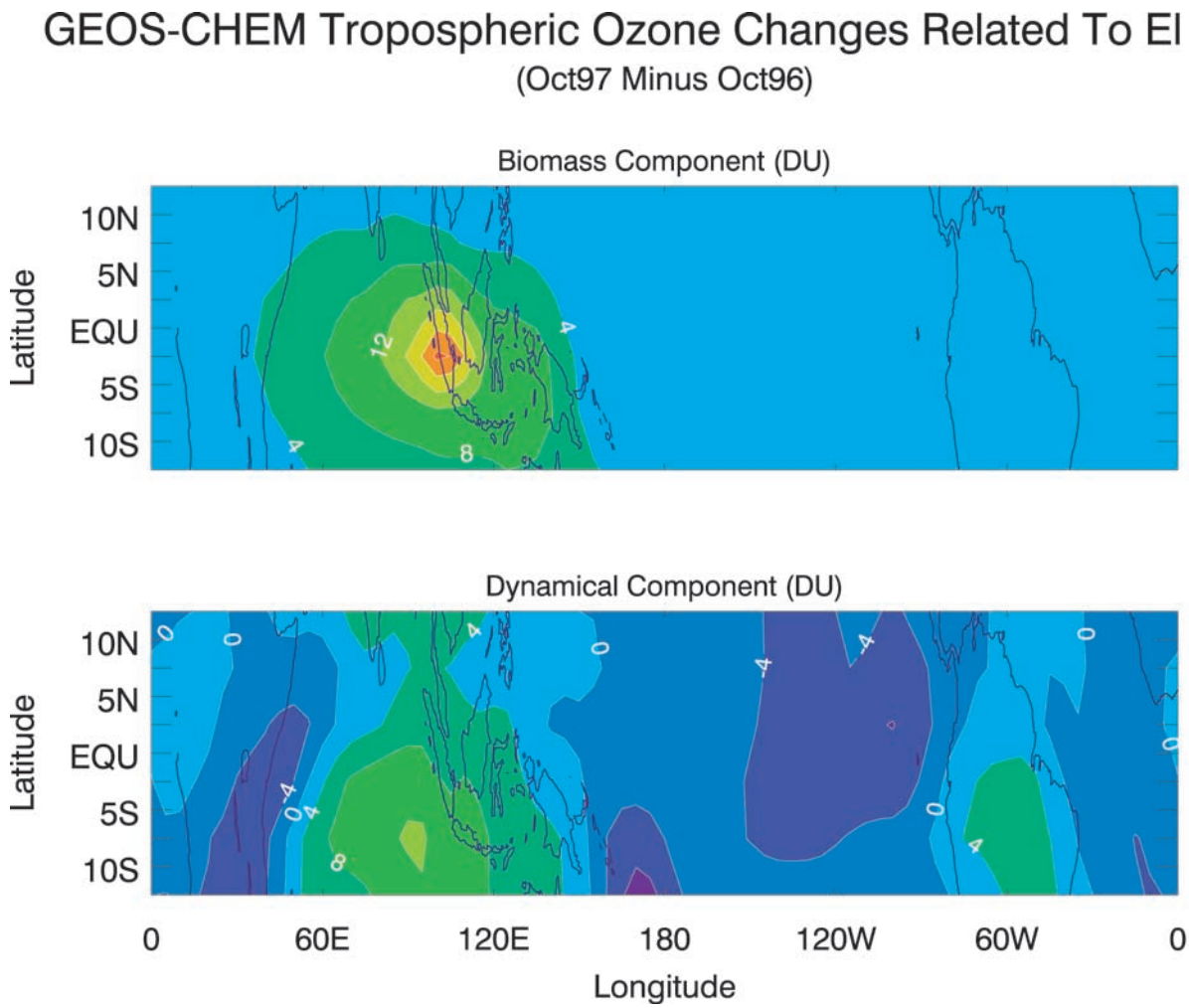

Figure 14. TCO anomaly inferred from the GEOS-CHEM model in the bottom panel of Figure 8 but with two different scenarios. (top) The first one takes into account the changes in biomass burning emission rates from October 1996 to October 1997 without changing the meteorological conditions. (bottom) The second scenario takes into account only the changes in meteorological conditions.

fires in the Indonesian region. *Thompson et al.* [2001], using tropospheric ozone and AI data, showed that decoupling of equatorial ozone and burning occurs over South America and Indonesia as well. Even in 1997 when intense biomass fires in August through October led to ozone pollution over the Indonesian maritime continent, *Thompson et al.* [2001] showed that subsidence associated with the onset of the El Niño and Indian Ocean dipole caused a 20 DU tropospheric ozone increase 5 months prior to the fires. Thus biomass burning may not be the main cause for an increase in tropospheric ozone.

[18] *Ziemke and Chandra* [1999] and *Chandra et al.* [1999] have shown that in addition to El Niño which primarily affects the eastern and western Pacific regions, the interannual variability in TCO is also influenced by the QBO and the solar cycle. Since dynamical components of El Niño tend to cancel out in the zonally averaged data and biomass burning is believed to be the dominant contributor to interannual variability in tropical NO_x emissions, the interannual variability in TCO should primarily reflect the effects of biomass burning, QBO, and solar cycle. These effects are clearly discernable in Figure 16 which shows monthly fluctuations in TCO with respect to climatology. They are area-averaged over 15°N–15°S (as in Figure 7) and smoothed using a 12-month digital low-pass filter to accentuate changes over a longer (QBO) timescale. The TCO time series show low-frequency oscillations which are characteristic of QBO as inferred from the zonal wind at 50 hPa measured at Singapore. In general, the TCO variability is out of phase with the 50 mbar zonal wind. An exception to this relationship occurs during 1997 and the 1991–1992 period when they tend to be in phase. The in phase relation during 1997 is clearly due to elevated ozone in the Indonesian region caused by biomass burning. Similar effects may have been present during 1991 and 1992 which were also El Niño years. Biomass burning in previous years, associated with African and Brazilian fires or El Niño related fires in the Indonesian region, may also have contributed to interannaual variability in TCO. However, their effects do not seem to be large enough to offset the

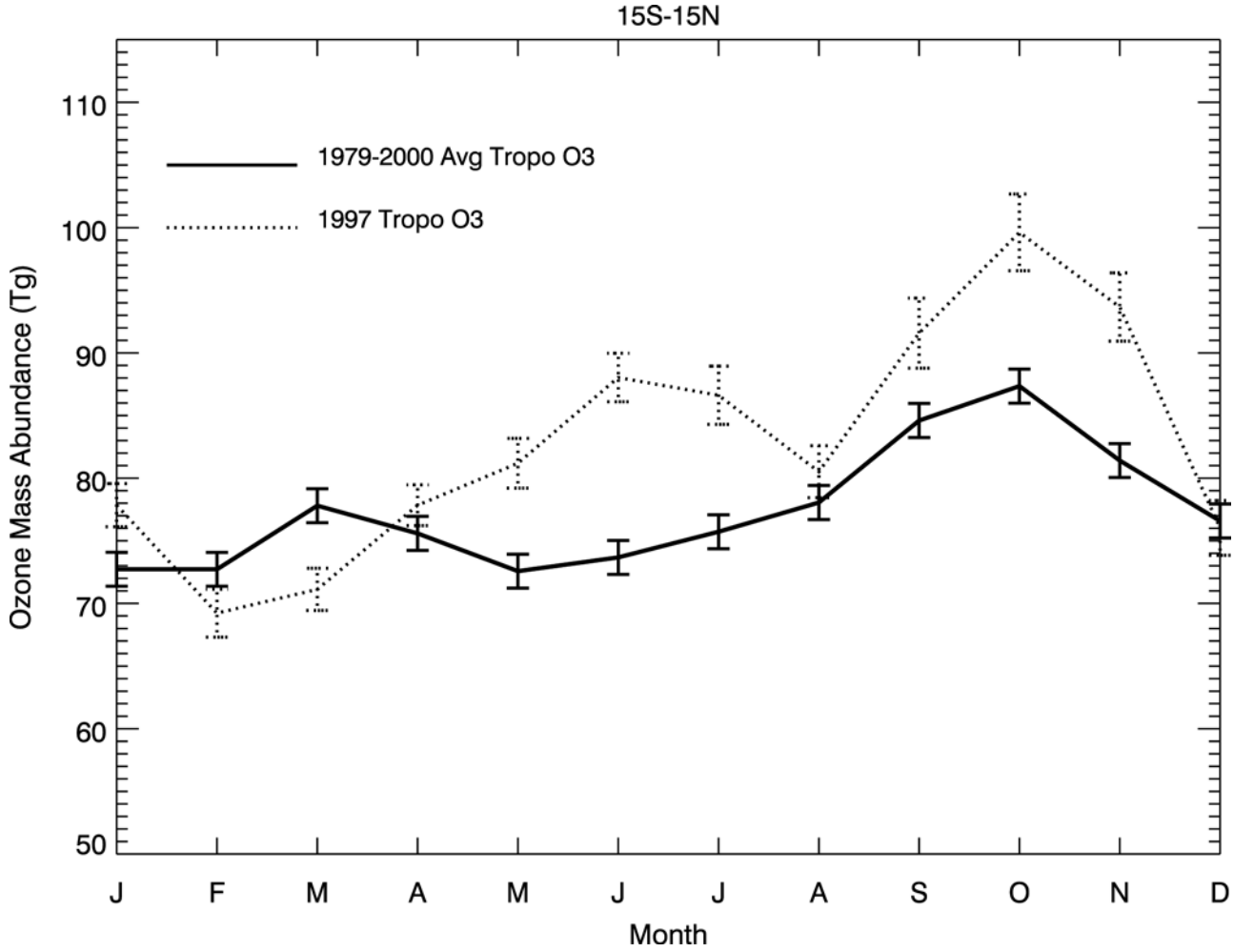

Figure 15. Comparison of the seasonal variation in TCO over the tropical region in 1997 with a climatology based on the 22 years (1979–2000) of the CCD database. Both data sets are area-averaged over the latitude band from 15°N to 15°S and are expressed in the units of teragrams (Tg; 1 Tg = 10^{12} g) to reflect the ozone mass abundance in the tropical troposphere.

out of phase relation between TCO and 50 mbar zonal wind.

[19] Figure 16 also suggests an out of phase relation of TCO time series with solar cycle as inferred from the 10.7 cm solar radio flux time series which is a traditional index of solar activity. Evidence for a solar cycle modulation of tropospheric ozone was shown by *Chandra et al.* [1999] for the marine atmosphere in the tropics. The magnitude of QBO and solar cycle components in Figure 16 can be estimated using a linear regression model (discussed by *Ziemke and Chandra* [1999]). For TCO the peak-to-peak amplitudes for the QBO and solar cycle components are 5.5 ± 3.8(2σ) and 5.6 ± 3.3(2σ).Tg, respectively. Assuming a mean value of 77 Tg, this corresponds to a peak-to-peak modulation of about 7% by both the QBO and solar cycle.

9. Summary and Conclusions

[20] In this paper we have studied the possible role of biomass burning in producing seasonal and interannual variabilities in tropospheric ozone in the tropics. Using TOMS-derived AI as an index of pyrogenic emissions associated with savanna and forest fires, we noted four major regions of significant biomass burning. Two of these regions lie north and south of the equator in the African subcontinent, and the other two regions lie in Brazil in South America and Indonesia in Southeast Asia. The African regions are associated with the dry periods which include December-January-February in the northern part and June-July-August in the southern part of Africa. The Brazilian fires are also associated with the dry season (July-August-September) in Brazil. However, they are not as persistent as the fires in the African regions. Notwithstanding the differences in biomass burning patterns of the three regions, the seasonal changes in TCO in these regions are essentially similar. Most of the observed seasonal characteristics are well simulated by the GEOS-CHEM global model of tropospheric chemistry. The main exception is the northern African region where modeled and observed TCO differ significantly. The model results also show good agreement with ozonesonde measurements both for tropospheric column ozone and ozone amount in the lower (below 500 hPa) and the upper (above 500 hPa) troposphere. The locations

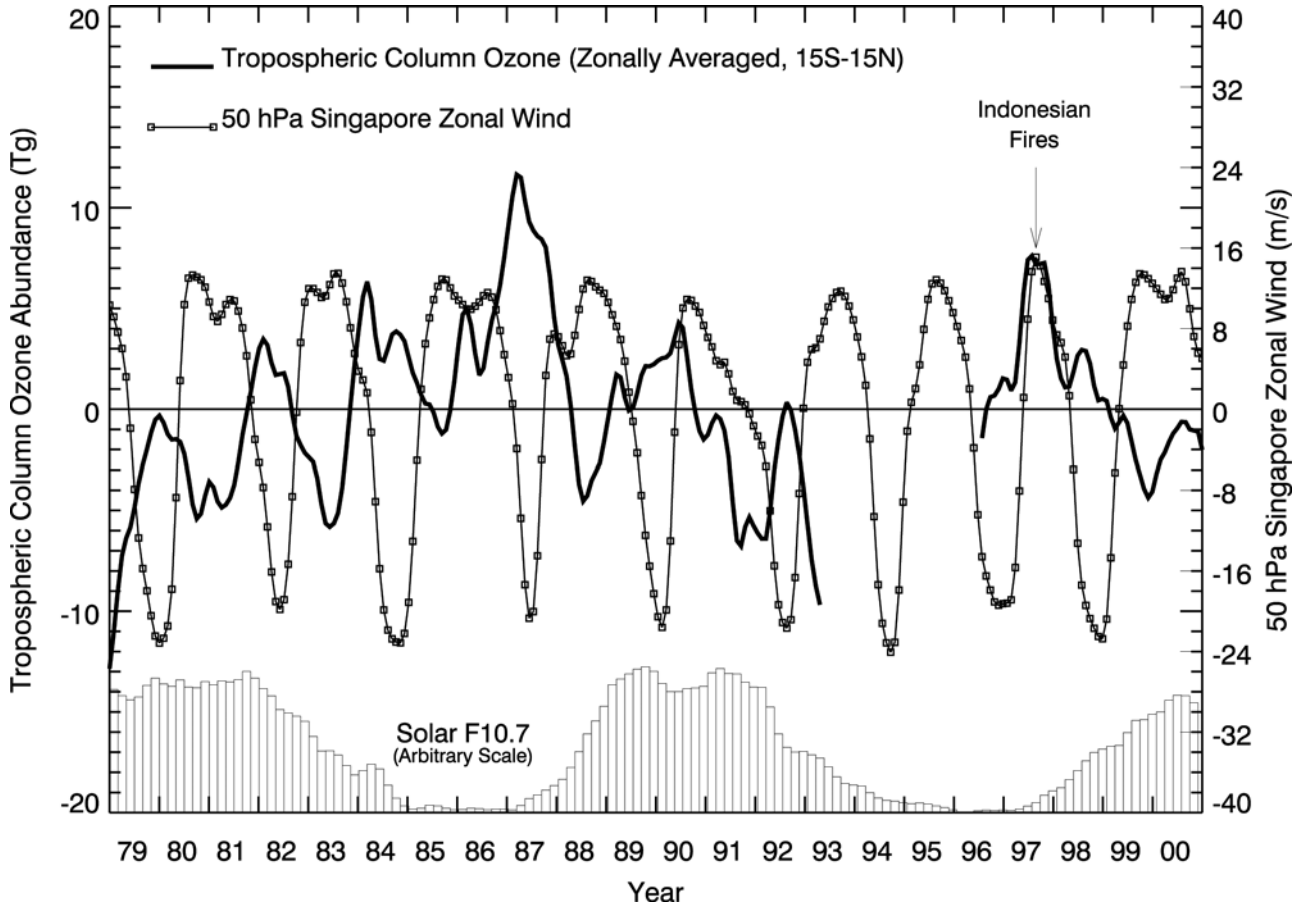

Figure 16. Tropospheric total ozone mass abundance (units in Tg) deseasonalized time series derived by area-averaging CCD column O_3 measurements in the latitude band 15°S to 15°N. The original deseasonalized monthly mean data were smoothed with a digital recursive low-pass filter with half frequency response at 12-month period. Shown in this figure are monthly mean zonal wind time series at 50 hPa at Singapore (small squares) and F10.7 cm monthly mean scaled solar flux (vertical bars). The F10.7 time series varies from around 70 to 200 (units 10^{22} W m^{-2} Hz^{-1}) from solar minimum to solar maximum.

chosen for these comparisons are Watukosek (8°S, 113°E) in the Indonesian region, Nairobi (1°S, 37°E) in the African region, and Samoa (14°S, 171°W) in the South Pacific region.

[21] In the Indonesian region the climatological values of AI are statistically not significant in any season except during September–October 1997 after the large-scale biomass burning which included both forest fires and Savanna fires. Our study has shown that TCO in this region began to increase before the onset of major fire events and reached peak values of 50–60 DU during September and October 1997. The elevated values of TCO persisted for several months after the fire events subsided. During the entire El Niño episode the increase in TCO was not limited to the biomass burning regions of Sumatra and Kalimantan in the Indonesian region but was extended over thousands of kilometers encompassing most of the western Pacific region. The increase in TCO in the western Pacific region was accompanied by a decrease in the eastern Pacific resembling a west-to-east dipole about the dateline. The model calculations suggest that both dynamically induced changes and the changes induced by biomass burning contributed almost equally to the observed enhancement in the tropospheric ozone over most of the Indonesian region.

[22] During September–October 1997 the net increase in TCO integrated over the tropical region 15°S–15°N is about 6–8 Tg over the climatological mean of about 77 Tg. The GEOS-CHEM model suggests that most of this increase may have been caused by the biomass burning in the Indonesian region since dynamical components of El Niño induced changes tend to cancel out in the area-averaged data. In addition to biomass burning, the interannual variability in the zonally averaged column ozone in the tropics is influenced by a number of factors including QBO and solar cycle.

[23] **Acknowledgments.** The GEOS-CHEM model was developed at Harvard University and was funded by the NASA Atmospheric Chemistry Modeling and Analysis Program. We gratefully acknowledge development of the GEOS-CHEM model by I. Bey, B. N. Duncan, A. M. Fiore, D. J. Jacob, Q. Li, H. Liu, J. A. Logan, A. C. Staudt, R. M. Yantosca, and R. M. Yevich. R. V. Martin was supported in part by a National Defense Science and Engineering Graduate Fellowship Program. The ozonesonde data for Watukosek were provided by Shuji Kawakami.

We also thank Kengo Sudo, Christina Hsu, and Paul Ginoux for helpful discussions.

References

Arino, O., and J.-M. Rosaz, 1997 and 1998 World ATSR Fire Atlas using ERS-2 ATSR-2 data, paper presented at Joint Fire Science Conference, U.S. Dep. of the Inter., Boise, Idaho, 15–17 June 1999.

Bey, I., D. J. Jacob, R. M. Yantosca, J. A. Logan, B. D. Field, A. M. Fiore, Q. Li, H. Y. Liu, L. J. Mickley, and M. G. Schultz, Global modeling of tropospheric chemistry with assimilated meteorology: Model description and evaluation, *J. Geophys. Res.*, *106*, 23,073–23,096, 2001a.

Bey, I., D. J. Jacob, J. A. Logan, and R. M. Yantosca, Asian chemical outflow to the Pacific: Origins, pathways, and budgets, *J. Geophys. Res.*, *106*, 23,097–23,114, 2001b.

Chandra, S., J. R. Ziemke, W. Min, and W. G. Read, Effects of 1997–1998 El Niño on tropospheric ozone and water vapor, *Geophys. Res. Lett.*, *25*, 3867–3870, 1998.

Chandra, S., J. R. Ziemke, and R. W. Stewart, An 11-year solar cycle in tropospheric ozone from TOMS measurements, *Geophys. Res. Lett.*, *26*, 185–188, 1999.

Chin, M., P. Ginoux, S. Kinne, O. Torres, B. Holben, B. N. Duncan, R. V. Martin, J. A. Logan, A. Higurashi, and T. Nakajima, Tropospheric aerosol optical thickness from the GOCART model and comparisons with satellite and sunphotometer measurements, *J. Atmos. Sci.*, *59*, 461–483, 2002.

Fenn, M. A., et al., Ozone and aerosol distributions and air mass characteristics over the South Pacific during the burning season, *J. Geophys. Res.*, *104*, 16,197–16,212, 1999.

Fiore, A. M., D. J. Jacob, I. Bey, R. M. Yantosca, B. D. Field, and J. Wilkinson, Background ozone over the United States in summer: Origin, trend, and contribution to pollution episodes, *J. Geophys. Res.*, *107*, 10.1029/2001JD000982, in press, 2002.

Fishman, J., V. G. Brackett, E. V. Browell, and W. B. Grant, Tropospheric ozone derived from TOMS/SBUV measurements during TRACE-A, *J. Geophys. Res.*, *101*, 24,069–24,082, 1996.

Fujiwara, M., K. Kita, S. Kawakami, T. Ogawa, N. Komala, S. Saraspriya, and A. Suripto, Tropospheric ozone enhancements during the Indonesian forest fire events in 1994 and in 1997 as revealed by ground-based observations, *Geophys. Res. Lett.*, *26*, 2417–2420, 1999.

Fujiwara, M., K. Kita, T. Ogawa, S. Kawakami, T. Sano, N. Komala, S. Saraspriya, and A. Suripto, Seasonal variation of tropospheric ozone in Indonesia revealed by 5-year ground-based observations, *J. Geophys. Res.*, *105*, 1879–1888, 2000.

Guenther, A., et al., A global model of natural volatile organic compound emissions, *J. Geophys. Res.*, *100*, 8873–8892, 1995.

Hauglustaine, D. A., G. P. Brasseur, and J. S. Levine, A sensitivity simulation of tropospheric ozone changes due to the 1997 Indonesian fire emissions, *Geophys. Res. Lett.*, *26*, 3305–3308, 1999.

Hsu, N. C., J. R. Herman, P. K. Bhartia, C. J. Seftor, O. Torres, A. M. Thompson, J. F. Gleason, T. F. Eck, and B. N. Holben, Detection of biomass burning smoke from TOMS measurements, *Geophys. Res. Lett.*, *23*, 745–748, 1996.

Hsu, N. C., J. R. Herman, J. F. Gleason, O. Torres, and C. J. Seftor, Satellite detection of smoke aerosols over a snow/ice surface by TOMS, *Geophys. Res. Lett.*, *26*, 1165–1168, 1999.

Jacob, D. J., et al., Origin of ozone and NO_x in the tropical troposphere: A photochemical analysis of aircraft observations over the South Atlantic basin, *J. Geophys. Res.*, *101*, 24,235–24,250, 1996.

Jacobson, M. Z., and R. P. Turco, SMVGEAR: A sparse-matrix, vectorized Gear code for atmospheric models, *Atmos. Environ.*, *28*, 273–284, 1994.

Kondo, Y., et al., Effects of biomass burning, lightning, and convection on O_3, CO, and NO_y over the tropical Pacific and Australia in August–October, *J. Geophys. Res.*, *107*, 10.1029/2001JD000820, in press, 2002.

Lelieveld, J., and F. J. Dentener, What controls tropospheric ozone?, *J. Geophys. Res.*, *105*, 3531–3551, 2000.

Levine, J. S., et al., The 1997 fires in Kalimantan and Sumatra, Indonesia: Gaseous and particle emissions, *Geophys. Res. Lett.*, *26*, 815–819, 1999.

Li, Q., D. J. Jacob, I. Bey, R. M. Yantosca, Y. Zhao, Y. Kondo, and J. Notholt, Atmospheric hydrogen cyanide (HCN): Biomass burning source, ocean sink?, *Geophys. Res. Lett.*, *27*, 357–360, 2000.

Li, Q., et al., Transatlantic transport of pollution and its effects on surface ozone in Europe and North America, *J. Geophys. Res.*, *107*, 10.1029/2001JD001422, in press, 2002.

Liu, H., D. J. Jacob, I. Bey, and R. M. Yantosca, Constraints from ^{210}Pb and ^{7}Be on wet deposition and transport in a global three-dimensional chemical tracer model driven by assimilated meteorological fields, *J. Geophys. Res.*, *106*, 12,109–12,128, 2001.

Martin, R. V., D. J. Jacob, J. A. Logan, J. R. Ziemke, and R. Washington, Detection of a lightning influence on tropical tropospheric ozone, *Geophys. Res. Lett.*, *27*, 1639–1642, 2000.

Martin, R. V., et al., Interpretation of TOMS observations of tropical tropospheric ozone with a global model and in situ observations, *J. Geophys. Res.*, *107*, 10.1029/2001JD001480, in press, 2002.

Marufu, L., F. Dentener, J. Lelieveld, M. O. Andreae, and G. Helas, Photochemistry of the African troposphere: Influence of biomass burning emission, *J. Geophys. Res.*, *105*, 14,513–14,530, 2000.

Moxim, W. J., and H. Levy II., A model analysis of tropical South Atlantic Ocean tropospheric ozone maximum: The interaction of transport and chemistry, *J. Geophys. Res.*, *105*, 17,393–17,415, 2000.

Palmer, P. I., D. J. Jacob, K. Chance, R. V. Martin, R. J. D. Spurr, T. P. Kurosu, I. Bey, R. Yantosca, A. Fiore, and Q. Li, Air mass factor formulation for spectroscopic measurements from satellites: Application to formaldehyde retrievals from GOME, *J. Geophys. Res.*, *106*, 14,539–14,550, 2001.

Price, C., and D. Rind, A simple lightning parameterization for calculating global lightning distributions, *J. Geophys. Res.*, *97*, 9919–9933, 1992.

Schubert, S. D., R. B. Rood, and J. Pfaendtner, An assimilated data set for Earth Science applications, *Bull. Am. Meteorol. Soc.*, *74*, 2331–2342, 1993.

Singh, H., et al., Distribution and fate of select oxygenated organic species in the troposphere and lower stratosphere over the Atlantic, *J. Geophys. Res.*, *105*, 3795–3805, 2000.

Sudo, K., and M. Takahashi, Simulation of tropospheric ozone changes during 1997–1998 El Nino: Meteorological impact on tropospheric photochemistry, *Geophys. Res. Lett.*, *28*, 4091–4094, 2001.

Thompson, A. M., K. E. Pickering, D. P. McNamara, M. R. Schoeberl, R. D. Hudson, J. H. Kim, E. V. Browell, W. W. J. H. Kirchhoff, and D. Nganga, Where did tropospheric ozone over southern Africa and the tropical Atlantic come from in October 1992?: Insights from TOMS, GTE/TRACE-A, and SAFARI-92, *J. Geophys. Res.*, *101*, 24,251–24,278, 1996.

Thompson, A. M., B. G. Doddridge, J. C. Witte, R. D. Hudson, W. T. Luke, J. E. Johnson, B. J. Johnson, S. J. Oltmans, and R. Weller, A tropical Atlantic paradox: Shipboard and satellite views of the tropospheric ozone maximum and wave-one in January–February 1999, *Geophys. Res. Lett.*, *27*, 3317–3320, 2000.

Thompson, A. M., J. C. Witte, R. D. Hudson, H. Guo, J. R. Herman, and M. Fujiwara, Tropical tropospheric ozone and biomass burning, *Science*, *291*, 2128–2132, 2001.

Thompson, A. M., et al., The 1998–2000 Southern Hemisphere Additional Ozonesondes (SHADOZ) tropical ozone climatology: Comparison with TOMS and ground-based measurements, *J. Geophys. Res.*, *107*, 10.1029/2001JD000967, in press, 2002.

Wang, Y., D. J. Jacob, and J. A. Logan, Global simulation of tropospheric O_3-NO_x-hydrocarbon chemistry, 1, Model formulation, *J. Geophys. Res.*, *103*, 10,713–10,725, 1998.

Wild, O., X. Zhu, and M. J. Prather, Fast-J: Accurate simulation of in- and below-cloud photolysis in tropospheric chemistry models, *J. Atmos. Chem.*, *37*, 245–282, 2000.

Yienger, J. J., and H. Levy, Empirical model of global soil-biogenic NO_x emissions, *J. Geophys. Res.*, *100*, 11,447–11,464, 1995.

Ziemke, J. R., and S. Chandra, Seasonal and interannual variabilities in tropical tropospheric ozone, *J. Geophys. Res.*, *104*, 21,425–21,442, 1999.

Ziemke, J. R., S. Chandra, and P. K. Bhartia, Two new methods for deriving tropospheric column ozone from TOMS measurements: The assimilated UARS MLS/HALOE and convective-cloud differential techniques, *J. Geophys. Res.*, *103*, 22,115–22,127, 1998.

Ziemke, J. R., S. Chandra, and P. K. Bhartia, A new NASA data product: Tropospheric and stratospheric column ozone in the tropics derived from TOMS measurements, *Bull. Am. Meteorol. Soc.*, *81*, 580–583, 2000.

Ziemke, J. R., S. Chandra, and P. K. Bhartia, Cloud slicing: A new technique to derive upper tropospheric ozone from satellite measurements, *J. Geophys. Res.*, *106*, 9853–9867, 2001.

P. K. Bhartia, S. Chandra, and J. R. Ziemke, NASA Goddard Space Flight Center, Code 916, Greenbelt, MD 20771, USA. (ziemke@jwocky.gsfc.nasa.gov)

R. V. Martin, Division of Engineering and Applied Sciences, Harvard University, Cambridge, MA 02138, USA.